

Critical currents of MgB₂ thin films deposited *in situ* by sputtering

S. L. Prischepa,* M. L. Della Rocca, L. Maritato,[†] and M. Salvato

INFN-COHERENTIA and Dipartimento di Fisica "E.R.Caianiello" - Università degli Studi di Salerno, Salerno, Italy

R. Di Capua, M. G. Maglione, and R. Vaglio

INFN-COHERENTIA and INFN-Sezione di Napoli, Dipartimento di Scienze Fisiche Università degli Studi di Napoli "Federico II," Napoli, Italy

(Received 26 July 2002; published 22 January 2003)

We have measured the temperature and magnetic field dependencies of the critical current density $J_c(H,T)$ in MgB₂ thin films, *in situ* deposited by sputtering. Three-dimensional point like normal core pinning was evidenced by measurements of the magnetic dependence of the pinning forces independently from the superconducting and structural quality of the investigated films. The analysis of the experimental data in terms of the collective pinning model has pointed out the presence of a crossover magnetic field from a single vortex to a small vortex bundle pinning regime. A ΔT_c pinning mechanism, i.e., a pinning associated with spatial fluctuations of the transition temperature, has been evidenced by the temperature dependence of this crossover field, in agreement with previous observations performed on MgB₂ bulk materials.

DOI: 10.1103/PhysRevB.67.024512

PACS number(s): 74.78.-w

The discovery of superconductivity in MgB₂ at a remarkably high transition temperature of ~ 39 K (Ref. 1) has led to intensive experimental and theoretical activities² to understand the basic phenomena of superconductivity and to investigate the pinning dynamics governing dissipative effects. Bulk MgB₂ samples have been largely analyzed, showing well-linked grains resulting in large critical current densities even in the presence of high external magnetic fields.³

In type-II superconductors with high values of the Ginzburg-Landau parameter κ , the most important elementary interaction between vortices and pinning centers is the so-called core interaction, arising from the influence of the parts of materials with the worse superconducting properties on the spatial variation of the superconducting order parameter. The core interaction is generally prevalent on the magnetic one, related to the presence of superconducting and nonsuperconducting interfaces parallel to the external field, which is very small in high- κ type-II superconductors.

MgB₂ bulk samples, with $\kappa \approx 20$,² have shown dissipative properties due to core pinning related to randomly distributed spatial variations of the transition temperature (ΔT_c pinning),⁴ in contrast to the case of high-temperature superconductors where the core interaction is associated with charge-carrier mean free path fluctuations (Δl pinning) mostly due to crystalline lattice defects.⁵

In situ thin films of MgB₂ have so far been fabricated using different deposition techniques,⁶ and have shown critical current density values higher than 10^{11} A/m².⁷ Due to the particular microstructures of thin films, the pinning mechanisms in these samples can be quite different from the bulk, and the study of their dissipative properties is interesting from the point of view of both the involved fundamental aspects and the future possible applications.

In this paper we report on measurements of the $J_c(H,T)$ dependencies in MgB₂ thin films, *in situ* deposited by sputtering on sapphire *R*-cut substrates.⁸ Our results indicate the presence of three-dimensional (3D) core pinning mechanism

and give evidence of ΔT_c pinning in agreement with what already observed in MgB₂ bulk samples.

MgB₂ thin films have been deposited *in situ* by planar magnetron sputtering, using a two step technique, in an ultra high-vacuum environment in the low 10^{-7} -Pa range. A full description of the fabrication procedure, including the deposition parameters, was reported elsewhere.⁸ The precursor deposition is performed at room temperature. After deposition, using a wobble-stick manipulator, the samples are placed *in situ* in a Nb box containing small amounts of Mg. The box is then well closed by a properly designed cap. At this point the heater is switched on and ramped up to 800 °C. An indium gasket guarantees a perfect sealing of the box. The process is therefore conducted in saturated Mg-vapor as in *ex situ* processes, giving high level film quality and reproducibility. The best films were obtained on *R*-cut sapphire substrates.

The film thickness, measured with a standard stylus profilometer, was about 0.6 μ m for the measurements reported here. An x-ray-diffraction pattern (Cu $K\alpha$), reported elsewhere,⁸ indicated a wide *c*-axis orientation of films deposited on MgO. Due to the substrate peak superposition, no structural evidence of *c*-axis orientation is available for films deposited on sapphire. The film surface morphology was investigated by atomic force microscopy and SEM showing granular features. The roughness on single grains is about 20 nm. The quite high room temperature resistivity values estimated using a standard four-probe geometry, are probably related to the granular structure of the films.⁹ Indeed, granularity affects the estimation of the "effective thickness," due to the limited contact area between the grains. Our best film had $T_c = 35$ K, $\Delta T_c = 0.5$ K (10–90 % criterion with a bias current of 100 mA) and a residual resistivity ratio of $(300 \text{ K})/(40 \text{ K}) = 1.6$. However samples with different superconducting properties have been analyzed.

In Fig. 1 the temperature dependence of the upper critical field H_{c2} , measured at the midpoint of the transition curves, both in the parallel and perpendicular direction with respect

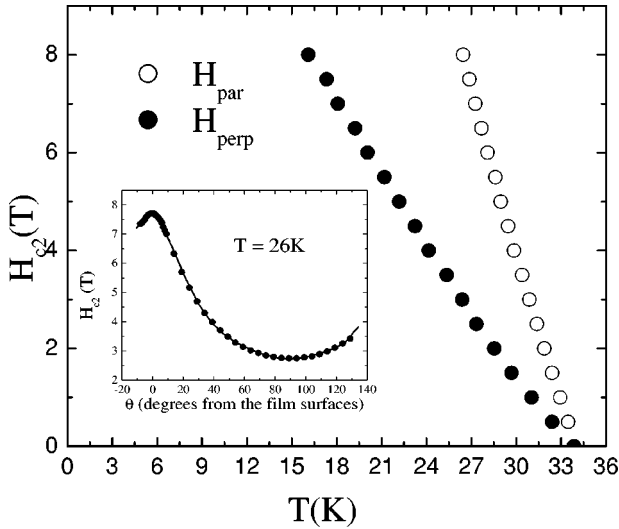


FIG. 1. Temperature dependence of the parallel and perpendicular upper critical fields for our best sample (sample A). In the inset, is shown the angular dependence of the upper critical field $H_c(\vartheta)$ at $T=26$ K. The solid line represents the Ginzburg-Landau formula for $H_c(\vartheta)$ (Ref. 11) obtained with $\gamma=2.7$.

to the film plane are reported up to a maximum field of 8 T for our best sample (sample A). As typically reported² both curves show a slight upward curvature close to T_c . From the critical field slope we can estimate $\xi_{\perp}(0)=2.3\pm 0.1$ nm and $\xi_{\parallel}(0)=5.7\pm 0.2$ nm, and an anisotropy ratio $\gamma=2.7$ (slowly temperature dependent). This value agrees fairly well with some current determinations on single crystals,¹⁰ indirectly proving the high quality and the c -axis orientation of our best films also when deposited on sapphire. A remarkable perfect fitting of the angular dependence of the critical field with the Ginzburg-Landau formula^{11,12} was possible at all temperatures. This is reported in the inset of Fig. 1 at $T=26$ K. Critical field measurements on lower quality thin-film samples resulted in lower anisotropy ratios (down to $\gamma=1.6$), possibly corresponding to a partial c -axis orientation.

For J_c measurements, after the deposition, a microbridge configuration was obtained using a scribing method.¹³ Typical widths of the microbridges were around $350\ \mu\text{m}$. J_c was measured using a standard four-probe technique along with a dc current source generator and adopting a threshold criterion of $1\ \mu\text{V}$. The magnetic field was applied perpendicular to the film surface.

In Fig. 2 we show the $J_c(H)$ curves for our best sample at six different temperatures. At low temperatures, the J_c values exceed $10^{10}\ \text{A/m}^2$ up to fields equal to 3.5 T, confirming high intergranular current flow in MgB_2 thin films.³ The inset in Fig. 2 presents the temperature dependence of the irreversibility field $H_{irr}(T)$, defined as the field at which the J_c values become lower than $10^6\ \text{A/m}^2$. The solid line in the inset, in close agreement with the data, is the law $[1-(T/T_c)^2]^{3/2}$, which is the typical behavior expected in the case of 3D flux creep.¹⁴ Pinning forces, defined as $F_p = \mu_0 H \times J_c$, can be calculated from the results of Fig. 2. In Fig. 3 we plot the reduced pinning force f versus the reduced magnetic field h ($f = F_p / F_{pmax}$, $h = H / H_{irr}$) at the same

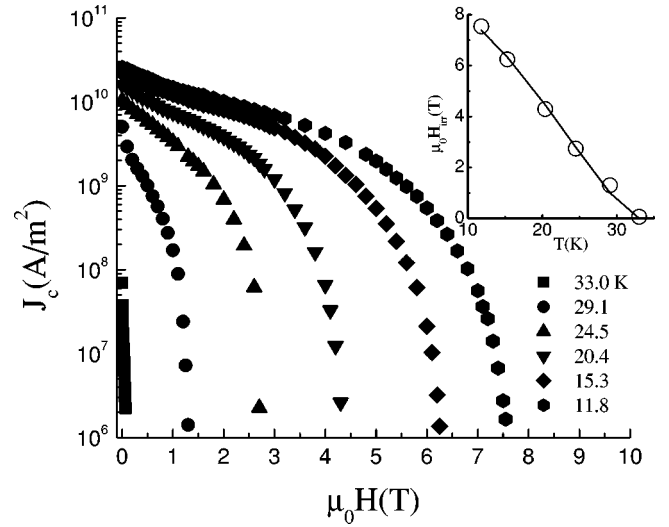


FIG. 2. $J_c(H)$ at different temperatures for sample A. In the inset is shown the temperature dependence of the irreversibility field for this sample. The solid line is obtained from the $[1-(T/T_c)^2]^{3/2}$ law.

temperatures of Fig. 2. H_{irr} is the field at which J_c vanishes and replaces H_{c2} when the value of the critical current is not determined by depairing effects.¹⁴ The curves exhibit a scaling behavior at $T < 30$ K, indicating, in this range of temperature, the presence of a single dominant pinning mechanism. In particular, the best fit of the curves (solid line in Fig. 3) is obtained with a $f(h)$ dependence given by $h^{1.1}(1-h)^{2.1}$, which is very close to the $h(1-h)^2$ dependence, expected in the case of point like normal core pinning centers.¹⁵ The presence of such a pinning mechanism is confirmed by the dependence of the maximum pinning force at a certain temperature F_{pmax} versus the irreversibility field H_{irr} , shown in

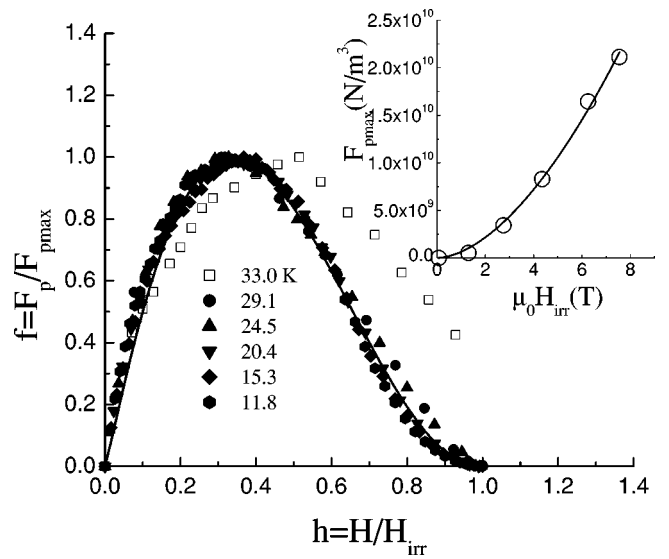


FIG. 3. Magnetic field dependence of the reduced pinning force $f(h)$, for sample A. The solid line represent the $f(h) \sim h^{1.1}(1-h)^{2.1}$ dependence. In the inset is shown the behavior of the maximum pinning force F_{pmax} vs the irreversibility field H_{irr} . The solid line is the law $F_{pmax} \approx H_{irr}^{\alpha}$ with $\alpha=1.8$.

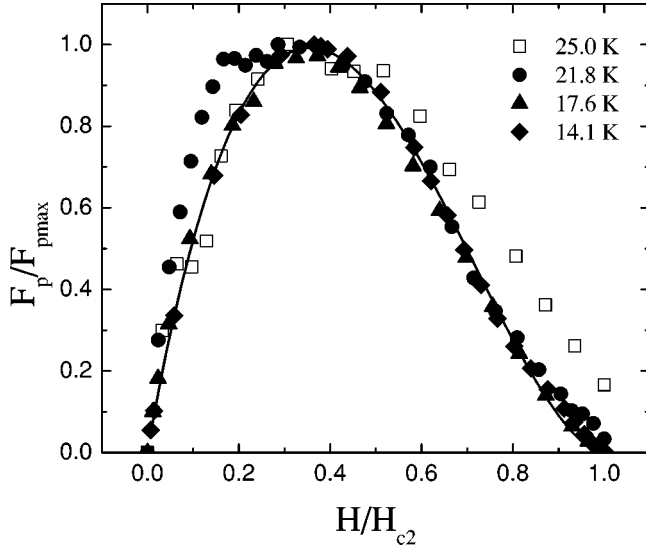


FIG. 4. Magnetic-field dependence of the reduced pinning force $f(h)$ for the sample with lower T_c (sample B). The solid line represent the $f(h) \sim h(1-h)^{1.8}$ dependence.

the inset to Fig. 3, which obeys the law $F_{pmax} \approx H_{irr}^\alpha$ with $\alpha = 1.8$, (solid line in the inset) close to $\alpha = 2$ derived by Dew-Hughes for the case of core normal point pinning.¹⁵

Similar results have been obtained also for other MgB₂ thin films with different superconducting properties. As an example, in Fig. 4 was report the $f(h, T)$ curves measured on a sample with $T_c = 28.0$ K (sample B), again showing a scaling behavior at temperatures below the critical one, well described by the dependence $h(1-h)^{1.8}$ (solid line in Fig. 4) close to that expected for core normal point-like pinning.

Given the presence of 3D core pinning in our MgB₂ thin films independently of their particular superconducting properties, it is important to distinguish between the case of ΔT_c and Δl pinnings. The three-dimensionality of the pinning phenomena in our samples, which show relatively low values of the anisotropy ratio,¹² has been confirmed by the analysis on the reduced pinning forces. In the frame of the collective pinning theory,¹⁶ valid for randomly distributed weak pinning centers, the elasticity or the plasticity of the flux-line lattice strongly influences the dissipative behavior. For a 3D elastic vortex lattice, it has been shown¹⁴ that the critical current density J_c is field independent in the presence of single-vortex pinning, i.e., for applied magnetic fields lower than a crossover field H_{sv} defined as

$$H_{sv} = \beta_{sv} \frac{J_{sv}}{J_0} H_{sv}, \quad (1)$$

where $\beta_{sv} \approx 5$, J_0 is the GL depairing current density, and J_{sv} is the critical current density in the single vortex-pinning regime. At higher fields, for $H > H_{sv}$, the pinning of small vortex bundles starts to be predominant and $J_c(H)$ follows an exponential law,¹⁴

$$J_c(H) \approx J_c(0) \exp\left\{-\left(\frac{H}{H_0}\right)^{3/2}\right\}, \quad (2)$$

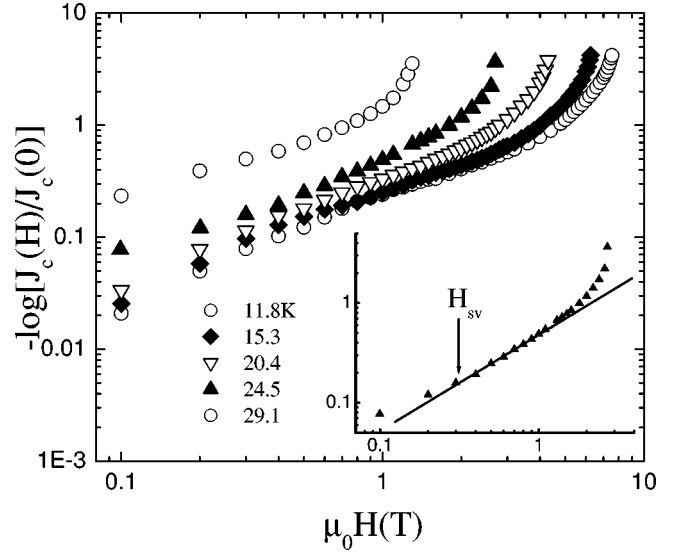


FIG. 5. Double logarithmic plot of $-\log[J_c(H)/J_c(0)]$ vs H for sample A at different temperatures. In the inset are pointed out the data at $T = 24.5$ K and the determination of the crossover field H_{sv} at this temperature.

where H_0 is a normalization parameter of the order of H_{sv} .

The experimental behavior shown in Fig. 2 for the $J_c(H)$ dependence, with an almost constant value of J_c at $H < 4$ T and a fast decrease at higher fields, can be described in terms of Eq. (2). As an example, in Fig. 5 we present the $-\log[J_c(H)/J_c(0)]$ versus H dependencies in a double logarithmic plot at $T < 30$ K for the data of Fig. 2. It is clear that Eq. (2), as expected, well describes the data for intermediate fields. The deviation at low fields is associated with the crossover from the single vortex pinning regime to the small bundle pinning regime, and allows to one estimate the field H_{sv} . The determination of H_{sv} is clear from the inset to Fig. 5, where we present the results at $T = 24.5$ K.

The discussion of the nature of the high field deviation from Eq. (2) is beyond the purposes of the present work. We point out that it could be probably related to large thermal fluctuations, as suggested by the 3D flux creep dependence observed for the $H_{irr}(T)$ curves in the inset to Fig. 2. Future work will concern this issue.

The crossover fields H_{sv} as a function of temperature, obtained using Eq. (2) and the aforementioned procedure, are shown in Fig. 6. As pointed out by Griessen *et al.*,⁵ the ΔT_c and Δl pinning mechanisms result in different temperature dependencies of the critical current density J_{sv} in the single vortex pinning regime. In particular, for the case of Δl pinning, one obtains a $J_{sv}(T)$ behavior given by $J_{sv} \propto ((1-t^2)^{5/2}(1+t^2)^{-1/2})$, with $t = T/T_c$, while for ΔT_c pinning the expected dependence is $J_{sv} \propto (1-t^2)^{7/6}(1+t^2)^{5/6}$. Inserting these two $J_{sv}(T)$ behaviors into Eq. (1), for the temperature dependence of the crossover field $H_{sv}(T)$ we obtain the expression

$$H_{sv} = H_{sv}(0) \left(\frac{1-t^2}{1+t^2}\right)^\nu, \quad (3)$$

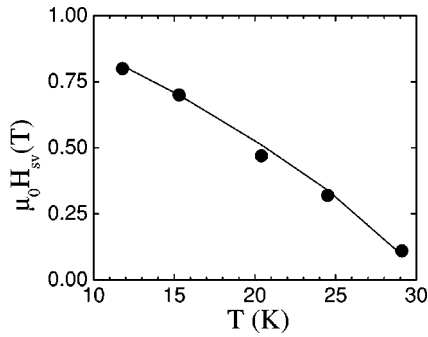


FIG. 6. Temperature dependence of the crossover field $H_{sv}(T)$ for sample A. The solid line is obtained from Eq. (3) with $\nu=2/3$.

where $\nu=2/3$ characterizes the case of ΔT_c pinning and $\nu=2$ that of Δl pinning.

Close to the critical temperature, the curvature associated to the ΔT_c case is positive, while that of the Δl pinning is negative. As it is clear from the data in Fig. 6, the $H_{sv}(T)$ behavior shows a positive curvature at $T < 30$ K, strongly indicating the predominance of the ΔT_c pinning mechanism in our thin-film samples. Moreover, the agreement among

our experimental points and Eq. (3) with $\nu=2/3$ is very good, as indicated by the solid line in Fig. 6 obtained from Eq. (3) using only one free fitting parameter, $H_{sv}(0)$.

In conclusion, we have measured the $J_c(H, T)$ dependencies in MgB_2 thin films, *in situ* deposited by sputtering. Independently of the superconducting and structural quality of the investigated films, the measurements of the magnetic dependence of the pinning forces have pointed out the presence of a 3D pointlike normal core pinning in the studied samples. Moreover, the analysis of the experimental data in terms of the collective pinning model has allowed the determination of a crossover magnetic field from a single vortex to a small vortex bundle pinning regime. The temperature dependence of this crossover field gives strong evidence of ΔT_c pinning, i.e., a pinning mechanism associated with spatial fluctuations of the transition temperature. These experimental findings are in agreement with previous observations performed on MgB_2 bulk materials, and indicate that in the analyzed samples pinning mechanisms typically present in thin film, such as for example surface or edge pinning, do not influence the dissipative phenomena.

This work was partially supported by the INFN ‘‘Eloisatron’’ Special Project.

*Also at State University of Computer Science and RadioElectronics, P. Brovka street 6, 220600, Minsk, Belarus.

†Electronic address: maritato@sa.infn.it

¹G.J. Nagamatsu, N. Nakagawa, T. Muranaka, Y. Zenitali, and J. Akimitsu, *Nature (London)* **419**, 63 (2001).

²C. Buzea and T. Yamashita, *Supercond. Sci. Technol.* **14**, R115 (2001).

³K. Kawano, J.S. Abell, M. Kambara, N. Hari Babu, and D.A. Cardwell, *Appl. Phys. Lett.* **79**, 2216 (2001).

⁴M.J. Qin, X.L. Wang, H.K. Lin, and S.X. Don, *Phys. Rev. B* **65**, 132508 (2002).

⁵R. Griessen, Wen Hai-hu, A.J.J. van Dalen, B. Dam, J. Rector, and H.G. Schnack, *Phys. Rev. Lett.* **72**, 1910 (1994).

⁶H.Y. Zhai, H.M. Christen, L. Zhang, C. Cantoni, M. Paranthaman, B.C. Sales, D.K. Christen, and D.H. Lowndes, *Appl. Phys. Lett.* **79**, 2603 (2001); S.R. Shinde, S.B. Ogale, R.L. Greene, T. Venkatesan, P.C. Canfield, S.L. Bud’ko, G. Lapertot, and C. Petrovic, *ibid.* **79**, 227 (2001); X.H. Zeng, A. Sukiasyan, X.X. Xi, Y.F. Hu, E. Wertz, Qi Li, W. Tian, H.P. Sun, X.Q. Pan, J. Lettieri, D.G. Schlom, C.O. Brubaker, Z.K. Liu, and Q. Li, *ibid.* **79**, 1840 (2001); G. Grassano, W. Ramadan, V. Ferrando, E. Bellingeri, D. Marr, C. Ferdeghini, G. Grasso, P. Manfrinetti, M. Putti, A.

Palenzona, and A. Chincarini, *Supercond. Sci. Technol.* **14**, 762 (2001); K. Ueda and M. Naito, *Appl. Phys. Lett.* **79**, 2046 (2001).

⁷K. Ueda and M. Naito (unpublished).

⁸R. Vaglio, M.G. Maglione, and R. Di Capua, *Supercond. Sci. Technol.* **15**, 1236 (2002).

⁹J.M. Rowell (unpublished).

¹⁰K.H.P. Kim, J.H. Choi, C.U. Jung, P. Chowdhury, H.S. Lee, M.S. Park, H.J. Kim, J.Y. Kim, Z. Du, E.M. Choi, M.S. Kim, W.N. Kang, S.I. Lee, G.Y. Sung, and J.Y. Lee, *Phys. Rev. B* **65**, 100510 (2002).

¹¹D.R. Tilley, *Proc. Phys. Soc. London* **86**, 289 (1965).

¹²M.G. Maglione, F. Chiarella, R. Di Capua, R. Vaglio, M. Salvato, L. Maritato, and S.L. Prischepa, *Int. J. Mod. Phys. B* (to be published).

¹³R.I. Chiao, M.J. Feldman, H. Ohta, and P.T. Parris, *Rev. Phys. Appl.* **9**, 183 (1974).

¹⁴G. Blatter, M.V. Feigel’man, V.B. Geshkenbein, A.I. Larkin, and V.M. Vinokur, *Rev. Mod. Phys.* **66**, 1125 (1994).

¹⁵D. Dew-Hughes, *Philos. Mag.* **30**, 293 (1974).

¹⁶A.I. Larkin and Yu.N. Ovchinnikov, *J. Low Temp. Phys.* **34**, 409 (1979).